EXPERIMENTAL DEMONSTRATION OF RESET CONTROL DESIGN[1]

Y. Zheng,[2] Y. Chait,[3] C.V. Hollot,[4] M. Steinbuch[5] and M. Norg[6]

ABSTRACT

Using the describing function method, engineers in the 1950's and 1960's conceived of novel nonlinear compensators in an attempt to overcome the performance limitations inherent in linear time-invariant (LTI) control systems. This paper is concerned with a subset of such devices called "reset controllers" which are LTI systems equipped with mechanism and law to reset its states to zero. This paper reports on a design procedure and a laboratory experiment in which the resulting reset controller provides better tradeoffs than LTI compensation. Specifically, we show that reset control almost doubles the level of sensor-noise suppression without sacrificing either disturbance-rejection performance or gain/phase margins. To the best of our knowledge, this is the first experimental demonstration of reset control in the literature.

---

[1] Supported in part by the National Science Foundation under Grant No. CMS-9313764. This support is appreciated.

[2] Formerly a Ph.D. research assistant, Mechanical & Industrial Engineering Department, University of Massachusetts, Amherst; Presently, a Servo Design Engineer, NeoMagic Corporation, Santa Clara, CA 95054; yzheng@neomagic.com.

[3] Associate Professor, Mechanical & Industrial Engineering Department, University of Massachusetts, Amherst, MA 01003, USA; chait@ecs.umass.edu.

[4] Associate Professor, Electrical & Computer Engineering Department, University of Massachusetts, Amherst, MA 01003, USA; hollot@ecs.umass.edu.

[5] Philips Centre for Manufacturing Technology, Mechatronics Department, P.O. Box 218, 5600 MD Eindhoven, The Netherlands; steinbuch_m@cft.philips.nl

[6] Philips Research Laboratories Building WY-p26, Prof. Holstlaan 4, 5656 AA Eindhoven, The Netherlands; norg_ml@cft.philips.nl

1. **INTRODUCTION**

For decades, control engineers have been stymied by the inherent performance limitations of linear time-invariant (LTI) control systems. In the 1950's and 1960's, they developed novel nonlinear compensators in an effort to overcome these constraints (for example, see Levinson (1958) and Foster *et al*. (1966)). This paper is concerned with a subset of these devices called "reset controllers" which are LTI systems with mechanism and law to reset their states to zero. A classic example of reset control is the so-called Clegg integrator which is a linear integrator whose output resets to zero whenever its input crosses zero (Clegg, (1958)). The motivation behind its development appeared to be its describing function $(1.69/w)\angle -38.1^{\circ}$ which favorably compares to the frequency response of a linear integrator $(1/w)\angle -90^{\circ}$. Indeed, its smaller phase lag hinted of a potential to circumvent the limitations imposed on LTI control systems by Bode's gain-phase relationship. However, twenty years passed before the work of Krishnan and Horowitz (1974) made an attempt to systematically incorporate a Clegg integrator into control system design, or, to generalize the resetting concept to higher-order systems as done in Horowitz and Rosenbaum (1975). Very importantly, these two papers showed via simulations that reset control could provide better tradeoffs than LTI control. They also showed that improved performance did not come from a "blind resetting" of an LTI controller, but from a distinct and intentional interplay between the reset mechanism and an appropriately designed LTI controller component.

Despite this demonstrated potential, reset control has remained an enigma on the modern control scene. One reason is that real-time implementation of reset control laws may have challenged the technologies of the 50-70's. Another reason may be the lack of sharp theoretical results to firmly establish the stability and performance properties of reset control systems. While some of our recent work is aimed at developing such results (see Hu *et al*. (1997) and Hollot *et al*. (1997)), the objective of this paper is to report on the experimental application of reset control conducted in the Ph.D. thesis of Zheng (1998). This experiment involves the speed control of a tape-drive system and introduces a modified version of the design procedure first developed in Horowitz and Rosenbaum (1975). The experiments confirm the earlier simulation studies and show that reset control can provide better tradeoffs than LTI compensation. Specifically, we show that reset control almost doubles the level of sensor-noise suppression without sacrificing either disturbance-rejection performance or gain/phase margins. In addition to providing one of the first experimental demonstrations of reset control in the literature, we hope this paper also provides renewed interest in the topic and supplies basis for further theoretical study.

The paper is organized as follows. In Section 2, we introduce the tape-speed control system and performance objectives that form the basis of our study. We argue that LTI control is not capable of meeting the given objectives. This sets the stage for the reset control design discussed in Section 3. Simulations show that reset control can alleviate these LTI limitations. In Section 4, we provide experimental verification of the reset control design. Finally, in Section 5 we discuss shortcomings in our knowledge of reset control which suggest areas for further study.

2. LTI DESIGN LIMITATIONS

This section introduces the specific control design problem studied in this paper and discusses the limitations of linear feedback control particular to this example. These tradeoff issues are well-known to control engineers and provide motivation for the reset control design presented in Section 3.

The feedback control design problem studied in this paper involves disturbance attenuation and sensor-noise suppression for a tape-speed control system. There are several subsystems in a tape-transport system such as the tape-speed and the tape-tension control subsystems. In this paper, we focus only on the tape-speed control subsystem consisting of a motor and belt-driven capstan wheel as shown in Figure 1.

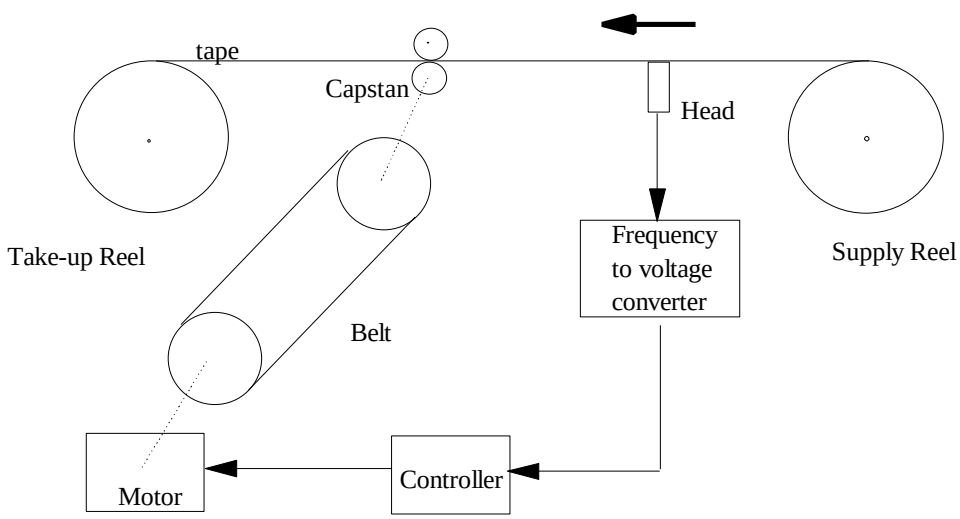

Figure 1: Schematic of the tape-speed control subsystem

The capstan's friction force pulls the tape past the read/write head and a frequency-to-voltage converter measures the tape-speed error relative to a 3.15 kHz master-tape speed. This tape-speed error signal is then fed back to the controller. Unlike conventional tape devices that use motor current as a measure of tape speed, this scheme measures tape-speed errors directly, thus providing a more accurate measurement of the physical variable to be controlled; see Pear (1967) and Mee and Daniel (1988) for details. A block diagram of the closed-loop tape-speed system is shown in Figure 2 where P represents the dynamics from the motor voltage u (volts) to the tape speed error y (volts) as measured by the frequency to voltage converter. System G represents the LTI controller, d is the lumped disturbance accounting for eccentricities and mechanical load variations and n models sensor noise. Eccentricities produce periodic disturbances related to the rotational

speed of various mechanical parts such as reels, capstan, etc. (see also Mathur and Messner, ((1998), while mechanical load variations are modeled by a broadband disturbance signal.

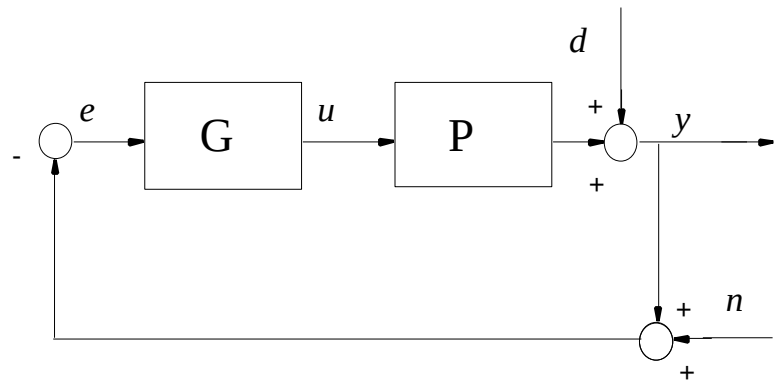

Figure 2: The closed-loop system configuration

The plant transfer function

$$P(s) = \frac{5.32e5(s^2 - 6.95e2s + 2.16e5)}{(s+14.02)\,(s^2 + 7.45e1s + 2.00e4)\,(s^2 + 2.03e2s + 3.28e4)}$$

was identified from a measured frequency response. In Figure 3 we compare the experimental and identified plant data which agree well.

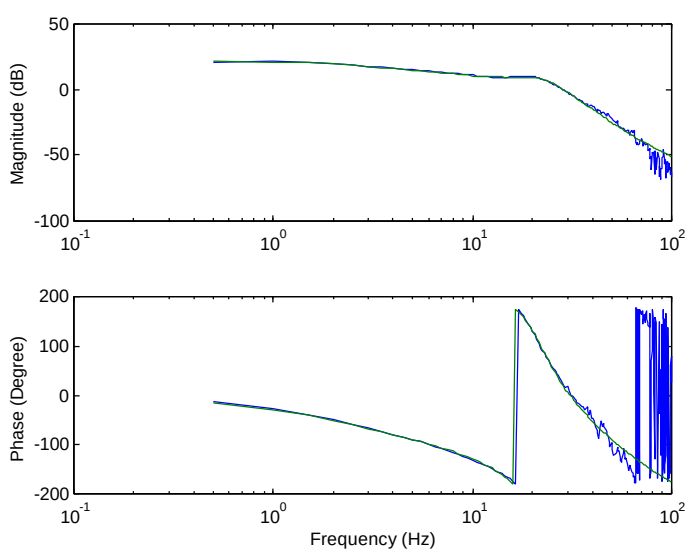

Figure 3: Comparison of experimental and identified plant frequency responses

In order to illustrate the LTI design limitations, we consider the following performance objectives. These objectives were chosen to illustrate the limitations of linear control and do no necessarily reflect realistic objectives for the tape-speed control system. In the following, the Fourier transform of a time-domain signal, say $y(t)$, is denoted by $y(j\omega)$. Similarly, the frequency response of a system P is denoted by $P(j\omega)$.

- **Disturbance rejection:** For all disturbances d satisfying $|d(j\omega)| \le 1$, the output y should satisfy $|y(j\omega)| \le 0.5$ for all $\omega \le 2(2\pi)$. Also, the response to a step disturbance should be zero in the steady state and limited to 20% overshoot.

- **Sensor-noise suppression:** For all sensor noise n satisfying $|n(j\omega)| \le 1$, the output y should satisfy $|y(j\omega)| \le 0.4$ for all $\omega \ge 10(2\pi)$.

To utilize frequency domain design techniques, we first translate the above specifications into constraints on the loop transfer function $L(j\omega) = G(j\omega)P(j\omega)$.

- **Disturbance rejection:** The disturbance-rejection specification can be described in terms of the sensitivity function:

$$\left|\frac{1}{1+L(j\omega)}\right| \le 0.5, \;\; \omega \le 2(2\pi)$$

  Zero steady-state error is achieved by requiring an integrator in the controller G.

- **(Gain/Phase) Margins**: Based on a second-order response assumption, we convert the overshoot specification into the following classical gain/phase margin constraint which also provides a reasonable degree of robustness against plant variations:

$$\left|\frac{L(j\omega)}{1+L(j\omega)}\right| \le 1.2, \;\; \omega \ge 0$$

- **Sensor-noise suppression:** The sensor-noise specification can be described in terms of the complementary sensitivity function:

$$\left|\frac{L(j\omega)}{1+L(j\omega)}\right| \le 0.4, \;\; \omega \ge 10(2\pi)$$

Based on our experience with controller implementation, we chose to design controllers directly from the plant frequency-response data. The Quantitative Feedback Theory (QFT) environment allows a designer to take advantage of such data, and, using the QFT Toolbox (Borghesani et. al. 1994), we attempted to design a controller to satisfy these performance objectives. However, it appears that LTI control may not be able to achieve these specifications. To see this, consider the QFT-derived controller

$$G_1(s) = \frac{14.85(s + 2.57e2)\,(s + 3.60)\,(s^2 + 19.21s + 2.29e2)\,(s^2 + 58.15s + 4.10e3)}{s\,(s^2 + 14.29s + 62.48)\,(s^2 + 215.3s + 1.272e4)\,(s^2 + 88.25s + 5.92e3)}$$

and the loop frequency response G_1P displayed on the Nichols chart in Figure 4.

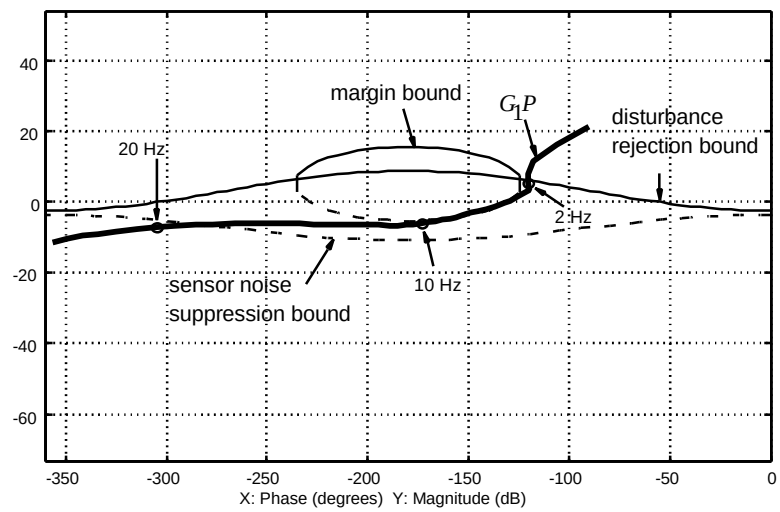

Figure 4: QFT bounds and the loop frequency response G_1P

The QFT bounds in Figure 4 precisely describe our performance specifications as constraints on the loop frequency response; see Zheng (1998) for details. Specifically, a solid-line bound requires the loop's response G_1P to lie above it to satisfy the specification. Conversely, a dashed-line bound requires the loop's response to lie on or below it to satisfy the specification. From Figure 4, we see that the loop G_1P satisfies the disturbance rejection and gain/phase margin specifications, but violates the sensor-noise suppression specification at 10 Hz; i.e., it does not lie below the bound. It seems unlikely that this design can be uniformly improved over the frequency range from 2-10 Hz. Indeed, since G_1P lies on the gain/phase margins boundary over the range 2-10 Hz and lies on the disturbance rejection bound at 2 Hz, then a loop magnitude reduction at 10 Hz must be followed by a deterioration in either the gain/phase margins or disturbance-rejection performance. This tradeoff is due to Bode's classical gain-phase relation which

links and constrains the amount of loop gain and phase change over a given frequency range.[7]

To illustrate this tradeoff, consider the "reshaped" loop G_2P where

$$G_2(s) = \frac{11.13\,(s+257.1)\,(s+3.606)\,(s^2+20.33s+216.3)(s^2+55.51s+3679)(s^2+75.74s+1.579e4)}{s\,(s+220.3)\,(s+36.49)\,(s^2+14.29s+62.48)(s^2+88.25s+5925)(s^2+125.7s+1.579e4)}$$

This loop was designed to satisfy both the sensor-noise suppression and disturbance rejection specifications as shown in Figure 5. As expected, decreasing the loop's magnitude at 10 Hz results in additional phase lag at smaller frequencies leading to violation of the gain/phase margins margin constraint.

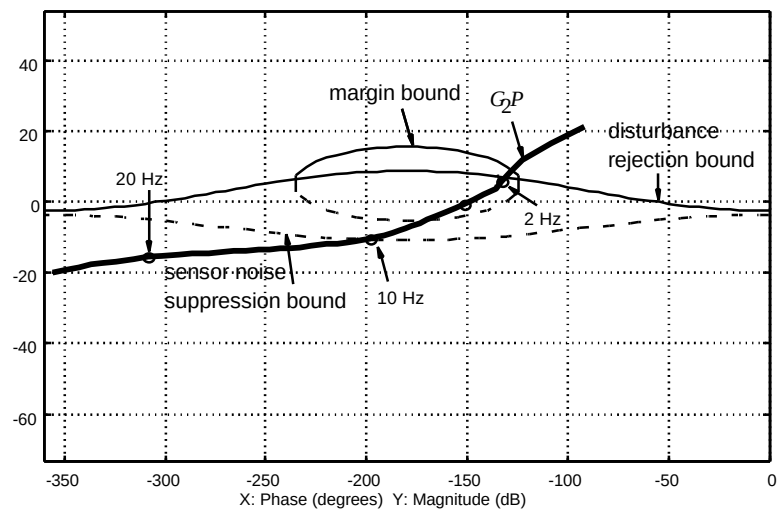

Figure 5: QFT bounds and the reshaped loop G_2P

These design tradeoffs can also be seen in the time domain. For example, consider the response y to both a step disturbance d and 10 Hz sinusoidal sensor noise n. The simulated responses for the two controllers G_1 and G_2 (Figure 6) verify the anticipated 50% increase in sensor-noise suppression for the second design.

[7] We attempted to improve performance by solving an H_∞ mixed-sensitivity problem wherein the complementary sensitivity and sensitivity weights were derived directly from the QFT-derived loop G_1P. The resulting H_∞-optimal design provided only marginal improvement over the frequency range 2-10 Hz.

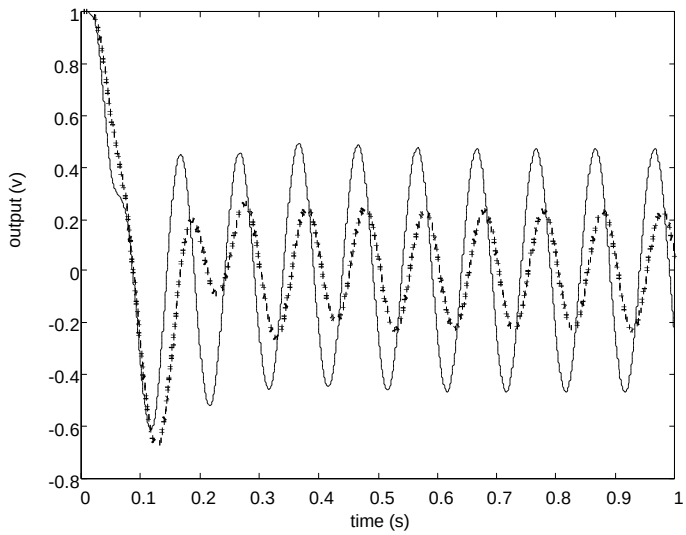

Figure 6: Simulated responses y to step disturbance d and sinusoidal sensor noise n corresponding to controllers G_1 (solid) and G_2 (dashed)

However, when the sensor noise is removed, the smaller gain/phase margins of the second design G_2P manifest itself as a 100% increase in overshoot; see Figure 7.

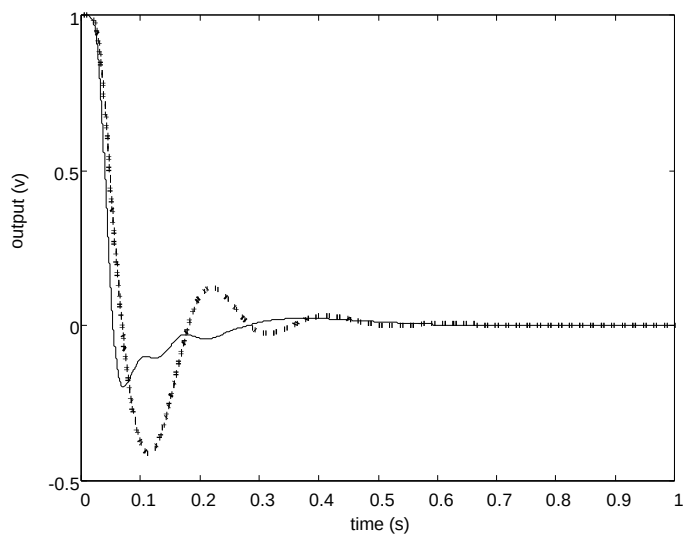

Figure 7: Simulated responses y to a step disturbance d corresponding to controllers G_1 (solid) and G_2 (dashed)

In summary, we have described a control problem where it is difficult, if not impossible, to satisfy the performance using an LTI controller. In the next section we turn to the class of reset controllers to provide better tradeoffs.

3. RESET CONTROL DESIGN

As demonstrated in the preceding section, LTI control systems are limited in their ability to make tradeoffs between competing performance objectives such as disturbance rejection, gain/phase margins and sensor-noise suppression. This motivates the study of reset controllers as a means for possibly improving this tradeoff. In this section we continue to study the control system problem introduced in the previous section and consider a reset controller composed of a cascade connection of a reset network G_R and a LTI controller G_L as shown in Figure 8.

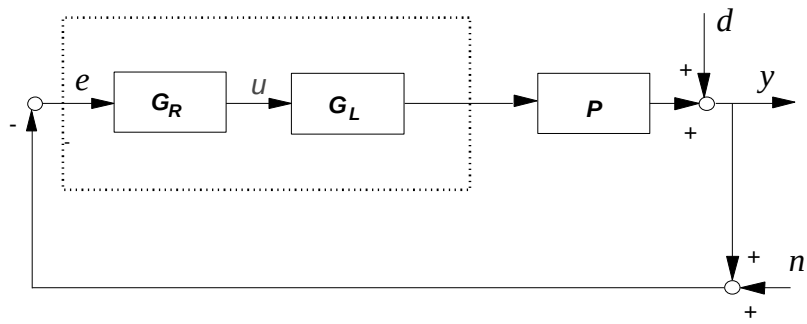

Figure 8: A reset control system

In this paper we take G_R to be a first-order reset element (FORE) as introduced in Horowitz and Rosenbaum (1975). This controller consists of a first-order linear filter with logic to reset the filter state to zero when its input e crosses zero. More precisely, the reset system G_R is described by the reset differential equation

$$\dot{x} = -bx + e; \qquad e \neq 0;$$

$$x = 0; \qquad e = 0;$$

$$u = x$$

where x is the state and where the filter's pole $b > 0$ is a design parameter. Essentially, G_R is a reset version of the linear element $1/(s+\mathrm{b})$. The linear part of the reset controller design is taken as

$$G_L(s) = G_2(s)\,(s+\mathrm{b})$$

As mentioned in the introduction, the design of the reset controller proceeds in two steps and involves interplay between the design of the linear element G_L and the reset network

G_R. The rationale introduced in Horowitz and Rosenbaum (1975) is to first design G_R and G_L so that the linear closed-loop response[8] satisfies both the disturbance rejection and sensor-noise suppression specifications (at the expense of violating the gain/phase margin constraint). In our case, this linear response is dictated by G_2 which, by design, meets the disturbance rejection and sensor-noise suppression requirements; see Figures 6-7 and the associated discussion. The next step involves choosing pole *b* to improve the overshoot response. Horowitz and Rosenbaum (1975) showed that resetting action reduces overshoot. Indeed, under a second-order assumption,[9] they related this overshoot to the crossover frequency ω_c [10] and phase margin of the linear design and the pole of the reset element as shown in Figure 9 where $M = \omega_c / b$. From Figure 5, the crossover frequency and phase margin of the linear loop $G_2 P$ is approximately 5 Hz (30 rad/sec) and 30° respectively. The design curve in Figure 9 indicates that *b* = 30 (*M* = 1) reduces the overshoot to 20% which satisfies the specification. We thus select *b* = 30 which completes the design. Finally, we note that in Horowitz and Rosenbaum (1975), *b* was required to be a pole of the linear design G_L. Our choice of forming $G_L(s) = (s+b)G_2(s)$ removes this constraint.

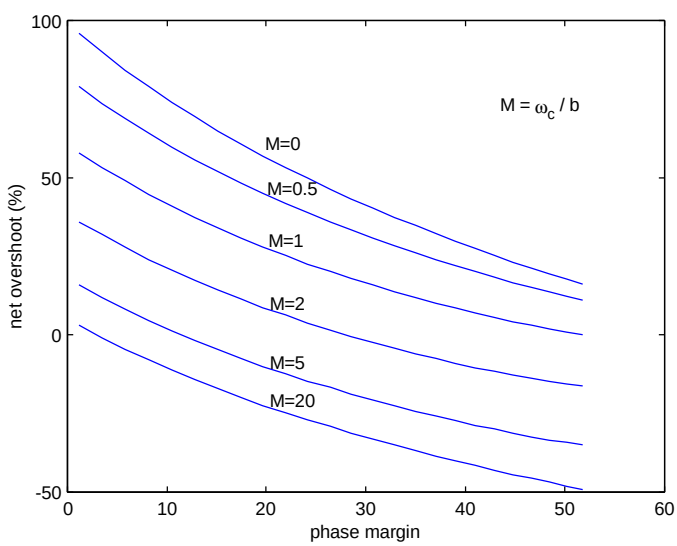

Figure 9: Relationship between overshoot of the reset control system, parameters of the

[8] By *linear closed-loop linear response* we refer to the control system's response *in the absence of resetting*. In the absence of resetting, the cascade connection of G_R and G_L reduces to G_2.

[9] In our context, this assumption amounts to the linear closed-loop transfer function $\frac{G_2 P}{1 + G_2 P}$ behaving like a standard second-order system $\frac{\omega_n^2}{s^2 + 2\zeta\omega_n s + \omega_n^2}$.

[10] The crossover frequency satisfies $|L(j\omega_c)| = 1$.

linear design and the reset pole *b*.

We now evaluate this reset controller design against our best linear design G_1 via simulation. In Figure 10 we compare the responses of these control systems to both step disturbance *d* and 10 Hz sinusoidal sensor noise *n*. In Figure 11 we show responses to only the step disturbance. The reset control design performs better by providing approximately 4-5dB more sensor noise attenuation (Figure 10) while displaying similar transient response (Figure 11). The reset control meets the performance specifications that linear control was unable to satisfy.

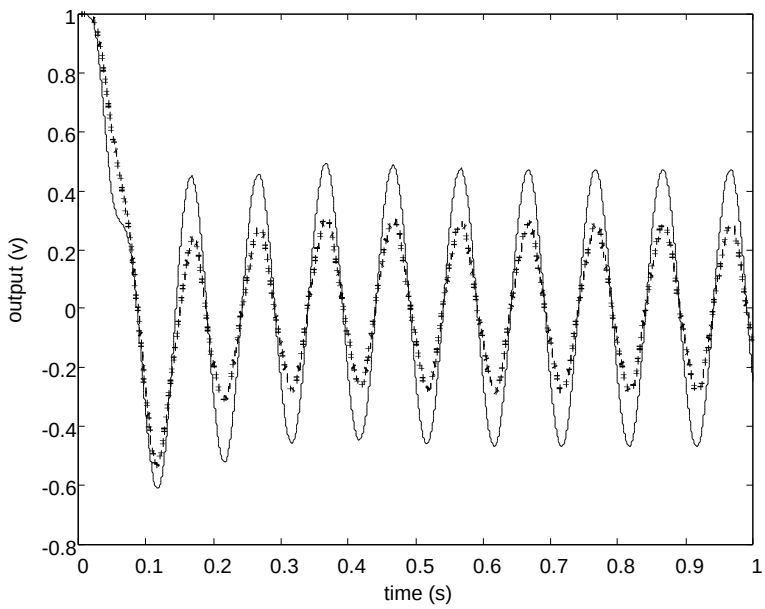

Figure 10: Simulated responses *y* to step disturbance *d* and sinusoidal noise *n* corresponding to controllers G_1 (solid) and reset with G_2 (dashed)

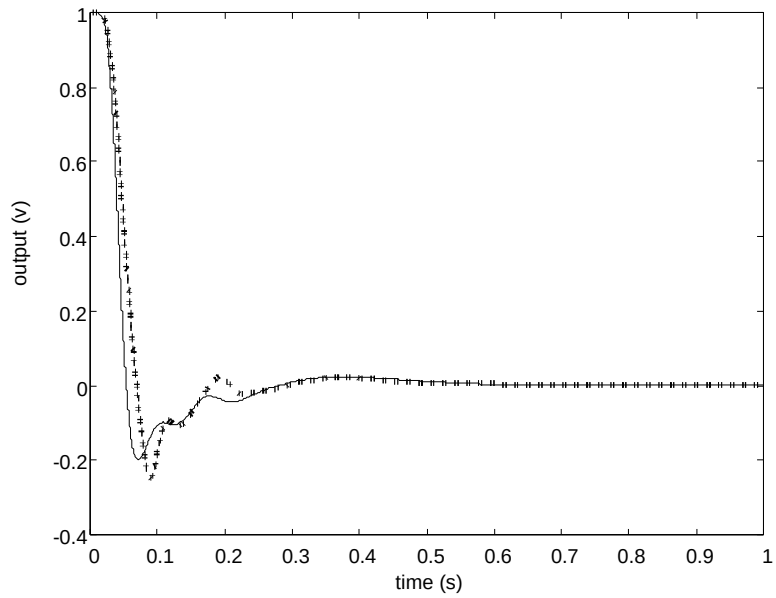

Figure 10: Simulated responses y to a step disturbance d corresponding to controllers G_1 (solid) and reset with G_2 (dashed)

Finally, to illustrate the design interplay required between the reset and linear elements, suppose we *blindly* implement the reset controller

$$\dot{x} = -30x + e, \qquad e \neq 0;$$

$$x = 0, \qquad e = 0;$$

$$u = x$$

with the linear element

$$G_L(s) = G_1(s)(s+30)$$

Clearly, there is no connection between the design of G_R and G_L. The simulations in Figures 12 and 13 show that improved performance does not occur. Moreover, the reduction of sensor noise in Figure 12 comes at the expense of sustained oscillations in Figure 13. Thus, improved performance does not come from blind resetting of an existing LTI controller such as G_1. Instead, it comes from distinct and intentional interplay between the reset mechanism and an appropriately designed LTI controller component such as G_2.

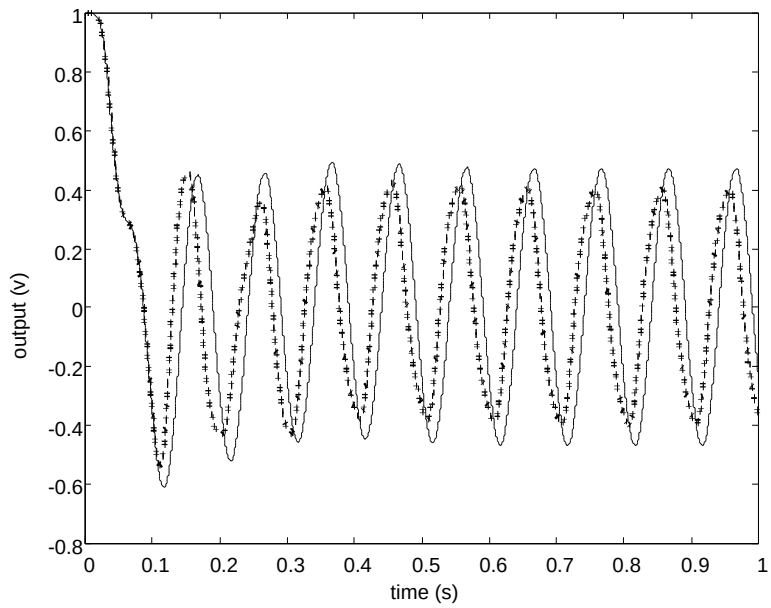

Figure 12: Simulated responses y to step disturbance d and sinusoidal noise n corresponding to controllers G_1 (solid) and reset with G_1 (dashed)

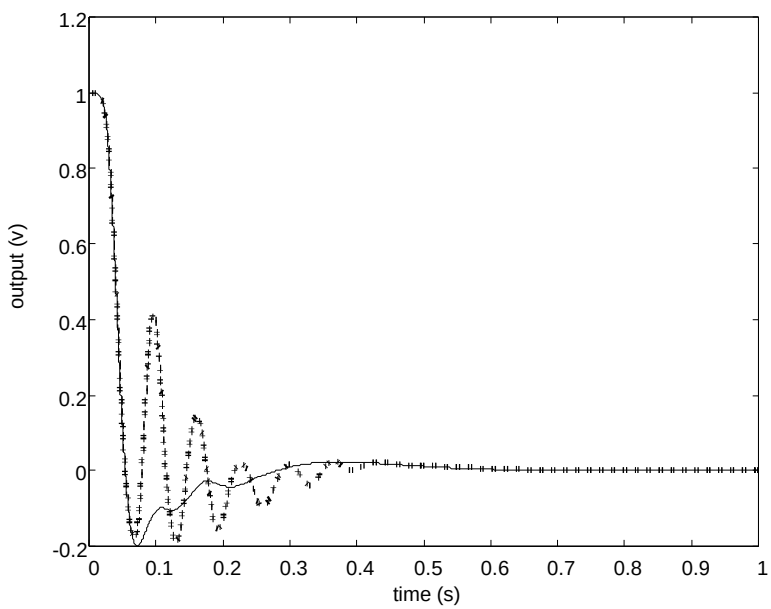

Figure 13: Simulated responses y to a step disturbance d corresponding to Controllers G_1 (solid) and reset with G_1 (dashed)

4. EXPERIMENTAL VERIFICATION OF RESET CONTROL

In this section we report on a real-time implementation of the reset controller designed and simulated in Section 3. The tape-drive system was described in Section 1 and together with the control hardware is shown in Figure 14. The controllers were digitally implemented on a TMS320C30 DSP system (32-bit floating point, 33 MHz 16-bit, ± 3.0 volts dynamics range A/D and D/A channels) using a 1kHz sampling rate. The controller integrator was implemented on a high-precision analog operational amplifier since it had larger dynamic range than digital implementation.

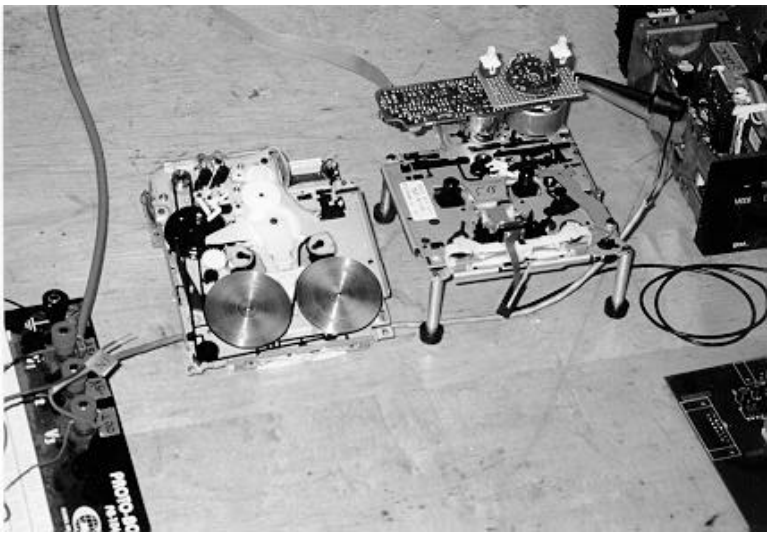

Figure 14: Experimental tape-speed system and control hardware

To simulate the step disturbance *d* and sensor noise *n*, we introduced a square-wave (with four-second period) and 10 Hz sinusoid respectively at the output of the frequency-to-voltage converter (see Figure 1). The response to this excitation was measured for both the linear G_1 and reset[11] controllers. The experimental results are shown in Figure 15. They show that both systems have similar disturbance rejection and transient behavior. However, as in the simulations, reset control improves sensor-noise suppression by 4-5dB.

[11] Recall that the reset controller is a cascade connection of a first-order reset element G_R and linear element G_2 as described in Section 3.

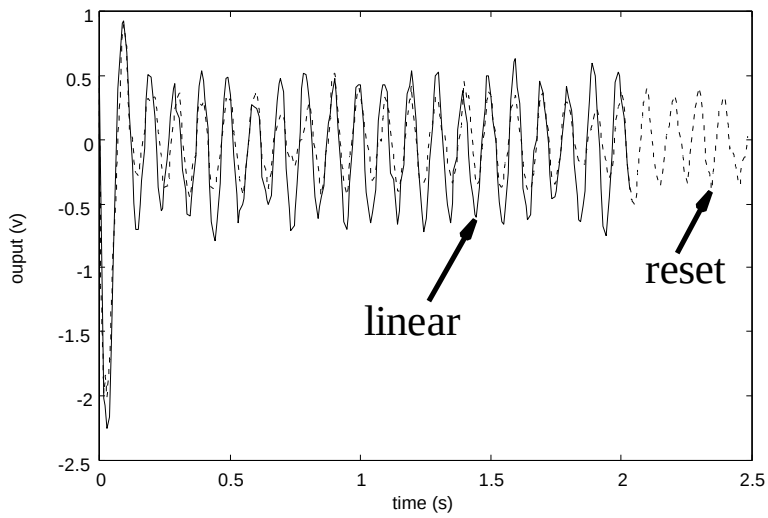

Figure 15: Experimental responses *y* to step disturbance *d* and sinusoidal noise *n* corresponding to linear G_1 (solid) and reset G_2 (dashed) controllers

Finally, we excited the tape-speed servo with filtered white noise *n* (50 Hz bandwidth) and measured the averaged voltage spectra of the frequency-to-voltage converter output for both the linear and reset control systems. The results, plotted in Figure 16, show that reset control provides an improvement in broadband sensor-noise suppression of 4-6dB over the 3-10 Hz frequency range

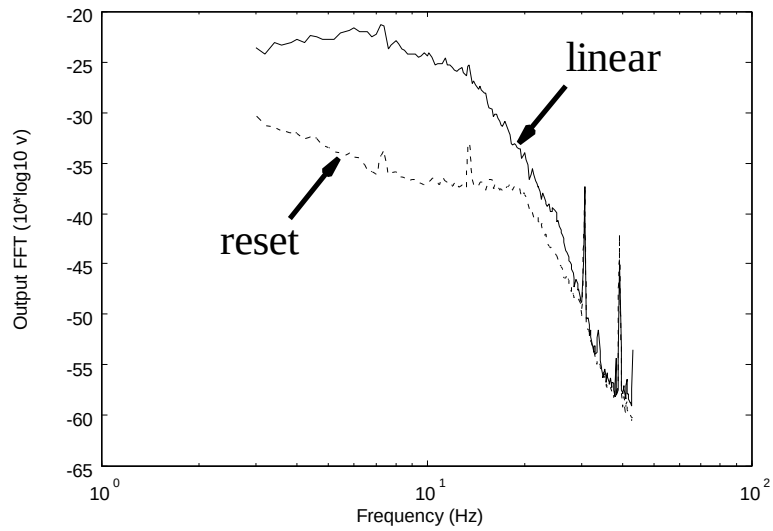

Figure 16: Spectra of tape-speed response to filtered white sensor noise (50 Hz bandwidth) - comparison between linear G_1 (solid) and reset G_2 (dashed) controllers

5. CONCLUSIONS

As demonstrated in this paper, a key element in reset control is the design of a base, linear control system with small gain/phase margins. The effect of introducing reset is to increase these margins without sacrificing the benefits derived from such linear controllers.[12] This is achieved by designing the reset action to improve transient performance. It was in this context that Horowitz and Rosenbaum (1975) made a connection between reset action, the linear control element and reduced overshoot. In fact, their design rule (see Figure 9) constitutes the *only concrete guideline* for presently designing reset controllers.[13] However, the scope of this guideline is limited. Specifically, the design rule guarantees only the following:

> If the linear closed-loop step system is second-order, then the first peak in the step response of the reset control system is reduced to an amount indicated in Figure 9.

Even if the linear step response happens to satisfy this second-order assumption, the design rule *does not guarantee*:

---

[12] These benefits include improved tradeoffs between competing objectives such as disturbance rejection and sensor-noise suppression which come at the expense of reduced gain/phase margins.

[13] It is interesting to note that describing functions, which provided the original motivation behind reset elements, do not play a role in this design technique.

Stable response to step disturbances. There is no guarantee that the response of the reset control system converges. Also, there is no guarantee on behavior when sinusoidal or random sensor noise is introduced.

Disturbance rejection and sensor noise suppression performance. There is no guarantee that the reset control system inherits the good performance properties of the linear design.

Overshoot reduction: There is no guarantee that the (global) maximum of the step response is reduced. The design rule guarantees only the *first peak* of the step response to be reduced.

In spite of these shortcomings, the ability of reset control to perform better than linear control (as demonstrated in this paper by both simulations and experiments) is a source of optimism. However, it appears that a number of theoretical questions need to be formulated and answered before reset control can be embraced as a viable control engineering tool. We have begun to address some of these issues in Hollot, *et al*. (1997) and Hu, *et al*. (1997).

6. REFERENCES

Borghesani, C., Chait, Y., and Yaniv, O., 1994, *The QFT Toolbox for MATLAB*, The MathWorks, Natick, MA.

Clegg, J.C., 1958, "A Nonlinear Integrator for Servomechanisms," *Trans. A.I.E.E.*, Part II, Vol. 77, pp. 41-42.

Foster, W.C., Gieseking, D.L. and Waymeyer, W.K., 1966, "A Nonlinear Filter for Independent Gain/phase (with Applications)," *Journal of Basic Engineering*, pp. 457-462.

Hollot, C.V., Zheng, Y., and Chait, Y., 1997, "Stability Analysis for Control Systems with Clegg Integrators," *Procs. IEEE Conference on Decision and Control*, San Diego, pp. 1717-1720.

Horowitz, I.M., 1963, *Synthesis of Feedback Systems*, Academic Press, New York, 1963.

Horowitz, I.M., and Rosenbaum, P., 1975, "Nonlinear Design for Cost of Feedback Reduction in Systems with Large Parameter Uncertainty," *International Journal of Control*, Vol. 21, pp. 977-1001.

Hu, H., Zheng, Y., Chait, Y., and Hollot, C.V., 1997, "On the Zero-Input Stability of Control Systems Having Clegg Integrators," *Procs. American Control Conference*, Albuquerque, pp. 408-410.

Krishnan, K.R., and Horowitz, I.M., 1974, "Synthesis of a Nonlinear Feedback System with Significant Plant-Ignorance for Prescribed System Tolerance," *International Journal of Control*, Vol. 19, pp. 689-706.

Levinson, E., 1958, "Gain-Phase Relations of Nonlinear Circuits," *IRE National Convention Record*, part 4, pp. 141-152.

Mathur, P.D., and Messner, W.C., 1998, "Controller Development for a Prototype High-Speed Low-Tension Tape Transport", *IEEE Trans. on Control Systems Technology*, Vol. 6, pp. 534-542.

Mee, C.D., and Daniel, E.D., 1988, *Magnetic Recording Handbook, Technology & Applications*, McGraw-Hill, New York.

Pear, C.B., Jr., editor, 1967, *Magnetic Recording in Science and Industry*, Reinhold Publishing Corporation, New York.

Zheng, Y., 1998, *Theory and Practical Considerations in Reset Control*, Ph.D. Dissertation, University of Massachusetts, Amherst.